

IMPACT OF DIAPHRAGMS ON SEISMIC RESPONSE OF STRAIGHT SLAB-ON-GIRDER STEEL BRIDGES

By Seyed Mehdi Zahrai¹ and Michel Bruneau,² Member, ASCE

ABSTRACT: Many steel bridges have suffered diaphragm (cross frame) damage during recent earthquakes. Diaphragms provide an important load path for the seismically induced loads acting on slab-on-girder steel bridges, but their impact on seismic response is still unclear in many ways. The relative role played by intermediate and end diaphragms in providing lateral load resistance, along with the consequences of diaphragm damage on bridge seismic response, has not been studied. This paper quantitatively investigates the impact of diaphragms on the seismic response of straight slab-on-girder steel bridges. Typical 20 to 60 m span slab-on-girder bridges with and without diaphragms are considered and studied through elastic and inelastic static push-over analyses. Two hand-calculation analytical models are proposed to evaluate their period, elastic response, and pseudospectral acceleration at first yielding. It is shown that a small end-diaphragm stiffness is sufficient to make the entire superstructure behave as a unit in the elastic range. However, a dramatic shift in seismic behavior occurs once an end diaphragm fractures, with a sizable period elongation, considerably larger lateral displacements, and higher propensity to damage owing to $P-\Delta$ effects. It is also found that the presence of intermediate diaphragms does not significantly influence the seismic performance of these types of bridges, in either the elastic or the inelastic range.

INTRODUCTION

Several steel bridges have collapsed or suffered significant damage during recent earthquakes such as the 1989 Loma Prieta (Earthquake 1990), 1994 Northridge (Astaneh-Asl et al. 1994; Earthquake 1994; Mitchell et al. 1995), and 1995 Kobe earthquakes (Bruneau et al. 1996). Although the potential seismic vulnerability of bridges designed and constructed at a time when seismic-resistant provisions were nonexistent or ineffective has long been recognized [e.g., Tseng and Penzien (1973) and Kawashima (1990)], these more recent failures have triggered considerable seismic evaluation and retrofit activities throughout North America and generated renewed research interest on that subject. However, most of the current knowledge in earthquake-resistant bridge design is based on past studies of concrete bridges, and may require adjustments to effectively capture the seismic behavior germane to steel bridges. One such aspect of this behavior is reviewed here.

Currently, in the literature on the seismic evaluation or design of bridges [e.g., Applied (1981), Buckle et al. (1986), Ontario (1991), and Standard (1994)], when the lateral period of a slab-on-girder bridge is determined, the superstructure (deck and girders) is modeled as an equivalent beam supported on columns and/or foundation springs. The effective transverse stiffness of this equivalent beam is calculated considering that the deck and girders act as a single cross section. While this approach is acceptable for concrete bridges and box-girder superstructures, it may not be for some types of existing slab-on-girder steel bridges. Typically, in such bridges, the concrete deck slab is supported on I-shape beams interconnected by a few discrete diaphragms, and the mechanism by which the seismically induced inertia forces at the concrete slab level will be transmitted to the girder bearings can be quite different from that assumed by the equivalent beam analogy. The mag-

nitude of this difference is tied to the effectiveness of the diaphragms, and can be quite large in bridges having flexible diaphragms. It is the objective of this paper to quantitatively investigate the lateral response of straight slab-on-girder steel bridges subjected to seismic lateral loads for various diaphragm conditions.

Here, a particular emphasis is placed on obtaining a proper representation of the superstructure's lateral stiffness, as this has a direct impact on bridge period and, consequently, on the intensity of earthquake excitation felt by the superstructure, bearings, and substructure. To achieve this, the behavior of bridges with and without any effective diaphragms is studied. Although the latter case may appear to be a theoretical situation, it is a model worth considering for the bridges having severely rusted diaphragms or with only nominal diaphragms (e.g., single channels bolted along their web as shown in Fig. 1) frequently encountered in eastern North America. Moreover, bridges having diaphragms with nonductile connection details can potentially become bridges without diaphragms once brittle failures develop at those connections. Comprehensive analytical expressions that capture the behavior germane to slab-on-girder steel bridges as a function of end-diaphragm characteristics are presented, and elastic and inelastic analyses are conducted to validate the proposed models.

PRELIMINARY INFORMATION

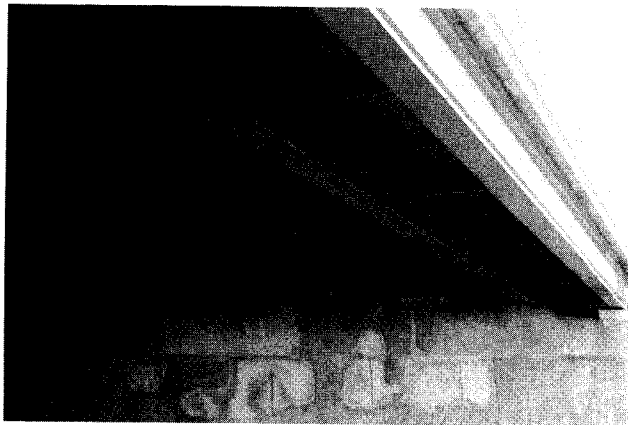
Diaphragm Design Requirements

Many bridge design codes require that slab-on-girder bridges be provided with end-span diaphragms as well as intermediate diaphragms (cross frames) at a spacing of no more than 7.6 m (Standard 1994) or 8 m (Ontario 1991). While these codes state that end diaphragms shall be proportioned to transmit all lateral forces to the bearings (and are designed by some departments of transportation to also serve as transfer members for jacks used to lift the superstructure during future bearing replacements), nothing is said about the role of the intermediate diaphragms. Although the intermediate diaphragms facilitate the construction process and stabilize the top compression flange of girders until the composite concrete deck is in place, no design guidance or detailing requirement is provided by these codes. In fact, even though some engineers have alleged that intermediate diaphragms can help evenly distribute the gravity and live loads among girders during service, recent research indicates otherwise (Azizinamini et al. 1995). As a result, diaphragm design has varied consid-

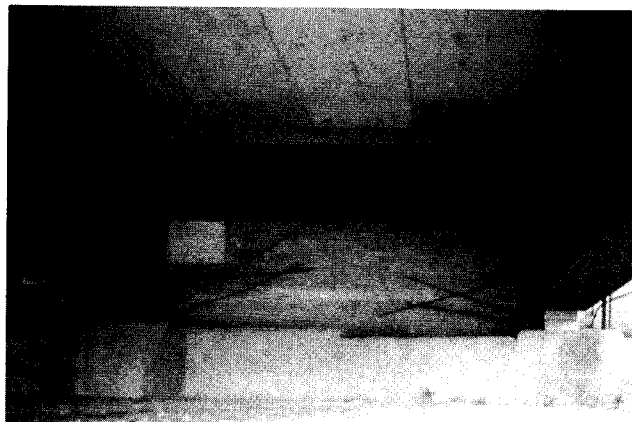
¹Postdoctoral Res. Assoc., Ottawa Carleton Earthquake Engrg. Res. Ctr., Dept. of Civ. Engrg., 161 Louis Pasteur, Univ. of Ottawa, Ottawa, Ont., Canada K1N 6N5. E-mail: szahrai@loki.nccs.net

²Prof., Ottawa Carleton Earthquake Engrg. Res. Ctr., Dept. of Civ. Engrg., 161 Louis Pasteur, Univ. of Ottawa, Ottawa, Ont., Canada K1N 6N5. E-mail: bruneau@genie.uottawa.ca.

Note. Associate Editor: Sashi K. Kunath. Discussion open until January 1, 1999. To extend the closing date one month, a written request must be filed with the ASCE Manager of Journals. The manuscript for this paper was submitted for review and possible publication on September 16, 1997. This paper is part of the *Journal of Structural Engineering*, Vol. 124, No. 8, August, 1998. ©ASCE, ISSN 0733-9445/98/0008-0938-0947/\$8.00 + \$.50 per page. Paper No. 16643.



(a)



(b)

FIG. 1. (a) Nominal Diaphragms Used in Slab-on-Girder Steel Bridge in Ottawa, Ont.; (b) Close-Up View of Nominal End Diaphragm of Slab-on-Girder Bridge in Quebec

erably in practice. [Note that specifications recently published by the American Association of State Highway and Transportation Officials (AASHTO-LRFD 1994) has replaced the arbitrary spacing requirement of diaphragms with a rational analysis that will improve practice in that regard.]

Diaphragms built with braces in X or chevron configurations, though popular for years, typically exhibit features undesirable from a seismic perspective, such as connection details that will fail prior to development of brace yielding. Moreover, these braces in older bridges were often designed to resist only wind loads and so have inadequate strength to resist earthquake loads. Not surprisingly, buckling and/or brittle failures of end-diaphragm members have been observed in recent earthquakes (Roberts 1992; Astaneh-Asl et al. 1994).

Interestingly, a very flexible type of diaphragm has been popular in some regions of eastern North America. As shown in Fig. 1, it consists of channels connected only by their webs

to the main girders. The effectiveness of such a diaphragm to transfer lateral loads is debatable. The much lower lateral stiffness by this type of diaphragm translates into a longer bridge structural period with correspondingly lower lateral forces, but larger drifts.

Description of Selected Bridges

Simply supported single-span bridges, each supported by hinged bearings on one abutment and expansion bearings on the other, are considered for this study. Although multispan, simply supported steel bridges are known to be more vulnerable to earthquakes (Diciceli and Bruneau 1995, 1996), the behavior of those more complex bridges can be modeled using the findings from the study reported here, by replacing each simply supported span with an equivalent beam whose mass and stiffness properties are selected to give the appropriate element stiffness using the equations developed hereafter.

The bridges designed by Diciceli and Bruneau (1995) are considered. To reflect the expected seismic performance of older existing highway steel bridges, these bridges were designed to be in compliance with the strength requirements of the 1961 edition of the American Association of State Highway Officials (AASHTO) code (*Standard* 1961). The characteristics of the bridges used in the current case study are listed in Table 1.

In all cases, 8-m-wide, two-lane straight bridges supported by four 300W grade steel girders spaced at 2 m center-to-center are considered. The bridge deck consists of a 200-mm-thick, 20 MPa concrete slab topped by 70 mm of asphalt. Finally, none of the bridges considered in this study have underside bracings; this was observed to be the case for those bridges in eastern North America having rather weak diaphragms.

SLAB-ON-GIRDER STEEL BRIDGES WITHOUT DIAPHRAGM

For bridges without diaphragm, preliminary analyses revealed that the concrete deck responded as a nearly rigid member in the transverse direction, irrespective of the pattern of the applied distributed lateral load. Hence, an equivalent static uniformly distributed load (UDL) applied at the deck level was deemed representative of the seismically induced inertia forces acting on this bridge structure. In the following, a generic load level corresponding to a pseudo-acceleration of 1g is considered. Obviously, all elastic analyses results presented in the following can be scaled as necessary.

The lateral response behavior of typical slab-on-girder steel bridges of various span lengths was first investigated using the program SAP90 (Wilson and Habibullah 1992). The resulting calculated first lateral period of vibration, resulting maximum drifts, and pseudospectral acceleration (PSa) required to produce first yielding are presented as a function of span length in Figs. 2(a-c), respectively (first yield being located in the

TABLE 1. Geometric and Structural Characteristics of Steel Bridge Considered in Case Studies*

| Span (m) (1) | Deck width (m) (2) | Number of girders (3) | Girder spacing (m) (4) | Slab depth (mm) (5) | Girder size and properties (6) | Mass (10^3 kg) (7) | I_w (10^{-8} m ⁴) (9) | I_b (10^{-8} m ⁴) (8) | I_D (m ⁴) (10) |
|-----------------|-----------------------|--------------------------|---------------------------|------------------------|-----------------------------------|--------------------------|---|---|---------------------------------|
| 20 | 8 | 4 | 2 | 200 | WWF800 × 184 | 126 | 0.111 | 56.25 | 1.322 |
| 30 | 8 | 4 | 2 | 200 | WWF1000 × 262 | 202 | 0.229 | 133.3 | 1.617 |
| 40 | 8 | 4 | 2 | 200 | WWF1200 × 333 | 286 | 0.341 | 160 | 1.797 |
| 50 | 8 | 4 | 2 | 200 | WWF1400 × 405 | 367 | 0.341 | 312.5 | 1.983 |
| 60 | 8 | 4 | 2 | 200 | WWF1600 × 496 | 465 | 0.341 | 485.3 | 2.212 |

* I_w , I_b , and I_D are the moments of inertia of girder web per unit length about bridge longitudinal axis, girder bottom flange about its strong axis, and superstructure about a vertical axis, respectively.

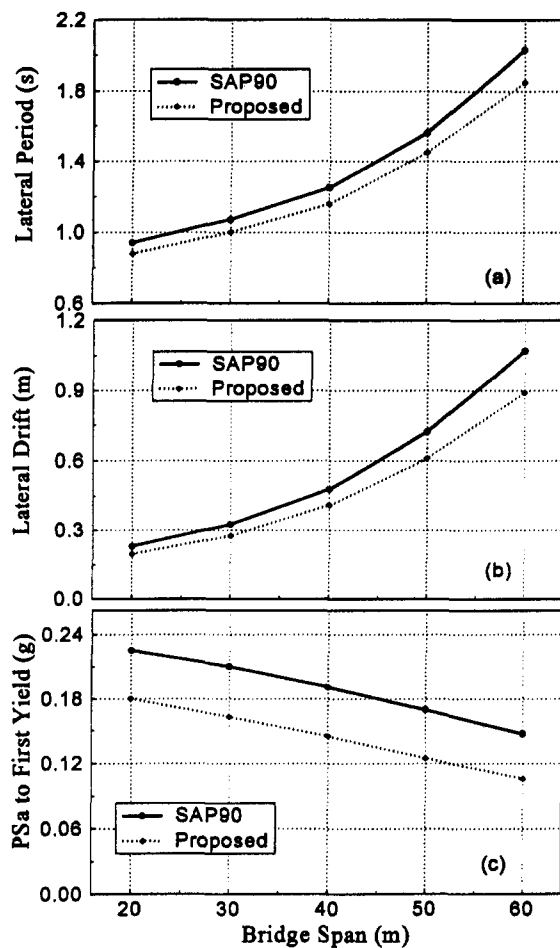


FIG. 2. Comparison of Results for Different Bridges (Laterally Simply Supported) Obtained by SAP90 and Proposed Model: (a) Lateral Period; (b) Lateral Drift; (c) Required PSa to Bring Bridge to First Yield

girder web, as described later). These terms vary nonlinearly as a function of span length in a complex manner because they depend on many other parameters that vary in the designed bridges of different lengths.

It is noteworthy that the resulting lateral periods and maximum lateral deflections are very large compared with values typically reported for slab-on-girder bridges in the literature, reflecting the extreme flexibility of the structural system in the absence of diaphragms. A typical deflected shape is presented in Figs. 3(a and b), where side views at support and along span show a big difference in relative displacements. Clearly, the concrete deck slab displaces laterally nearly as a rigid body, while the flexible steel girders twist and deform laterally as necessary spanning between the slab and the supports. Closer examination of the steel beams reveals that they are most severely distorted near the supports; indeed, in each girder, the bearing supports are the only points that can counteract the lateral pull of the web to bring the lower flange under the slab. This visual observation of behavior has led to the formulation of the proposed model described in the following section. Note that, throughout this study, it was found preferable to model the entire bridge (i.e., all girders and full width of deck) to capture the correct seismic behavior. Furthermore, calculated stresses and strains in the concrete deck slab are small and not reported in this paper.

Proposed Model for Calculation of Period, Elastic Response, and PSa to First Yielding

Clearly, based on the above description of behavior, an appropriate model should consider the displacement of the deck

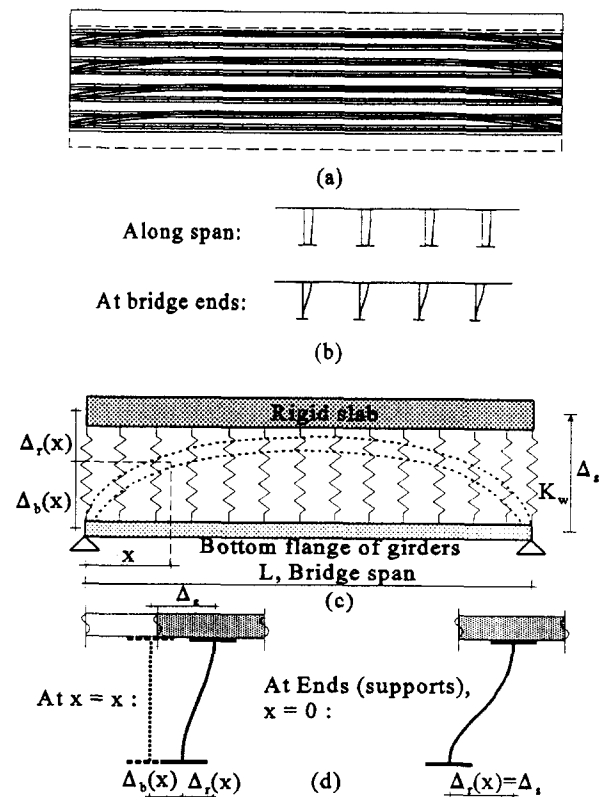


FIG. 3. SAP90 Deformed Shapes for Typical Bridges without Diaphragm: (a) Plan View; (b) Side Views and Schematic of Simplified Model without Diaphragm; (c) Plan View; (d) Side Views

slab relative to the bottom flange of girders, the web of girders providing a stiffness link between these two components. As a result, stresses in the webs vary greatly along the span. In fact, in each girder, web stresses will be largest at both ends where the bottom flange is restrained by the bearings, and will be minimum at midspan. Figs. 3(c and d) show a schematic simplified model of this behavior for slab-on-girder steel bridges without diaphragms.

Analytical expressions to calculate the lateral period and deformations of a bridge can be developed using this model. For that purpose, since the relative displacement between the deck slab and the lower flanges of the girders plays a key role on behavior, it is convenient to define a relative displacement term, $\Delta_r(x)$, as

$$\Delta_r(x) = \Delta_s - \Delta_b(x) \quad (1)$$

where Δ_s and $\Delta_b(x)$ are the displacements of the slab and bottom flanges of the girders, respectively. Since the deck slab nearly behaves as a rigid diaphragm in its plane, Δ_s is assumed to be constant in this case. In light of the above observations, the behavior of a bridge without diaphragms was found to closely resemble that of a beam on elastic foundation, and that mathematical model was adopted here. In this analogy, the girder bottom flange and web, respectively play the roles of the beam on a flexible surface and the springs of uniform stiffness. Therefore, the differential equation describing the bottom flange relative lateral displacement, $\Delta_r(x)$, is

$$EI_b \frac{d^4 \Delta_r(x)}{dx^4} = -k_w \Delta_r(x) \quad (2)$$

where E is modulus of elasticity; I_b is the bottom flange moment of inertia about its strong axis; and k_w is the web stiffness per unit length. If the bridge deck and bottom flanges can be assumed to remain always horizontal (i.e., without rotation about the bridge's longitudinal axis), the web stiffness can be modeled as

$$k_w = \frac{12EI_w}{h_w^3} \quad (3)$$

where I_w is the web moment of inertia per unit length about the longitudinal axis of the bridge; and h_w is the web height between top and bottom flanges. In reality, SAP90 analyses of the bridges under lateral seismic loading reveal that while the deck remains relatively horizontal, the bottom flanges rotate and the above assumption makes the bridge model slightly too stiff. However, this is of little consequence in most cases, as will be demonstrated later. The classical solution of (2) is

$$\Delta_r(x) = C_1 \sin \beta x \sinh \beta x + C_2 \sin \beta x \cosh \beta x + C_3 \cos \beta x \sinh \beta x + C_4 \cos \beta x \cosh \beta x \quad (4)$$

where C_1 to C_4 are constant coefficients depending upon the boundary conditions; and β is

$$\beta = \sqrt[4]{\frac{k_w}{4EI_b}} \quad (5)$$

If both ends of each bottom flange are assumed to be simply supported in the transverse direction, then $\Delta_r(x)$ is

$$\Delta_r(x) = \frac{2R_s \beta \cosh \beta x \cos \beta(L-x) + \cosh \beta(L-x) \cos \beta x}{k_w \sin \beta L + \sinh \beta L} \quad (6)$$

where R_s is the support reaction resulting from bridge lateral loading tributary to one girder (based on the UDL applied at the deck level); and L is the bridge span. To obtain the fundamental lateral structural period, the generalized mass and stiffness, m^* and K^* , can be computed from the following:

$$m^* = \int_0^L \left(\left(m_s + \frac{n_g m_g}{2} \right) \Delta_s^2 + \frac{n_g m_g}{2} \Delta_b^2(x) \right) dx \quad (7)$$

$$K^* = n_g \left(\int_0^L \frac{12EI_w}{h_w^3} \Delta_r^2(x) dx + \int_0^L EI_b \Delta_b^2(x) dx \right) \quad (8)$$

where n_g is the number of girders; and m_s and m_g are slab and girder's masses per unit length, respectively. Knowing that $\Delta_r = \Delta_s$ at the supports ($x = 0$), R_s can be obtained as a function of Δ_s from (6). For simplicity, since the mass of the girders is much smaller than that of the slab, m_g and m_s can be lumped together, and

$$m^* = \int_0^L \frac{m}{L} \Delta_s^2 dx = m \Delta_s^2 \quad (9)$$

where m is the entire bridge mass per unit length. In all cases, the lateral period of the bridge is given by

$$T = 2\pi \sqrt{\frac{m^*}{K^*}} \quad (10)$$

The resulting periods and maximum drifts calculated according to this procedure are plotted in Figs. 2(a and b) and compare well with the more accurate SAP90 results. In percentages, the difference between the results obtained using the proposed model and SAP90 increases as span length increases. For example, the lateral period and drift obtained by the proposed model are, respectively 6% and 12% less than those given by SAP90 for the 20 m span bridge, whereas these differences increase to 9% and 17% for the 60 m span bridge. Note that periods are more closely approximated by this procedure than maximum displacements (beware that the vertical axis for the period graph does not start at zero).

Figs. 4 and 5 compare the lateral displacements of the bottom flange obtained using SAP90 and the proposed procedure, for 20 m and 60 m span bridges. In each case, three different

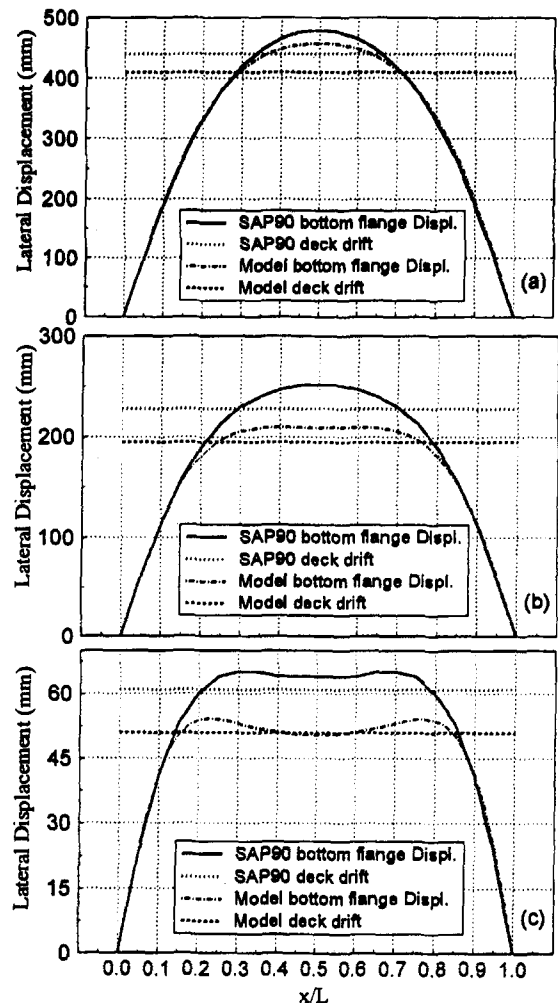


FIG. 4. Comparison of Girder Bottom Flange Displacements Obtained by SAP90 and Proposed Model for 20 m Span Bridge (Simply Supported Laterally), Respectively, for Girder Web Thickness of (a) 8 mm; (b) 11 mm Corresponding to WWF800 × 184 in Original Design; (c) 20 mm

web thicknesses were considered to illustrate sensitivity of response to this parameter. Clearly, the model works better for thinner webs and shorter spans. Although not shown on any figure, this is also true for the calculated fundamental period of vibrations, but with a lesser sensitivity. For example, the difference between the periods obtained by SAP90 and the proposed model for bridges having an 8 mm girder web thickness is only 4%, compared with 6% for the case with 11 mm girder web thickness.

The differences observed above are mainly a consequence of neglecting bottom flange torsional rotations in the proposed model. As shown in Fig. 6, where girder bottom flange twists are normalized per 100 mm drift, maximum normalized flange twist increases along with web thickness for a given bottom flange stiffness. Thus, for a thinner web, the normalized bottom flange twist is smaller, and the results of the proposed model and SAP90 [Figs. 4(a) and 5(a)] are in better agreement.

Maximum stresses in the girder webs will occur at the bridge end and can be calculated by assuming full fixity at top and bottom of the girder webs. This stress is given by

$$\sigma_{\max} = \frac{M_{w,\max} t_w}{2I_w} = \left(\frac{6EI_w}{h_w^2} \Delta_s \right) \frac{t_w}{2I_w} = \frac{3Et_w}{h_w^2} \Delta_s \quad (11)$$

where $M_{w,\max}$ is the maximum bending moment in the web, and Δ_s refers to maximum deck displacement. This equation is used to calculate the PSA required to bring the bridge to first yielding. Results are presented and compared with SAP90

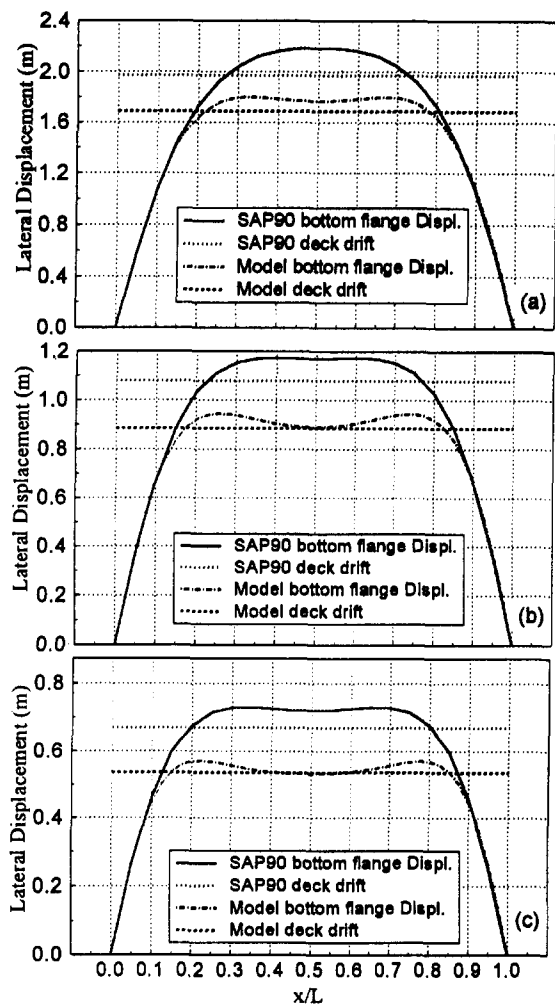


FIG. 5. Comparison of Girder Bottom Flange Displacements Obtained by SAP90 and Proposed Model for 60 m Span Bridge (Simply Supported Laterally), Respectively, for Girder Web Thickness of (a) 12 mm; (b) 16 mm Corresponding to WWF1600 × 496 in Original Design; (c) 20 mm

results in Fig. 2(c). Neglecting bottom flange rotation is conservative in this case.

Interestingly, if the bottom flange of each girder is assumed laterally fixed at one end (which would be the case if bearings at that end were prevented from moving in the longitudinal direction of the bridge), then (6) describing the relative deflection, $\Delta_r(x)$, would become

$$\begin{aligned} \Delta_r(x) = & \beta \frac{2R_2 \sin \beta L - R_1 \sinh \beta L}{k_w \cosh \beta L} \sin \beta x \sinh \beta x \\ & + \frac{R_1 \beta}{k_w} (\sin \beta x \cosh \beta x - \cos \beta x \sinh \beta x) \\ & + \beta \frac{2R_2 \cos \beta L + R_1 \cosh \beta L}{k_w \sinh \beta L} \end{aligned} \quad (12)$$

where R_1 and R_2 are reactions at fixed and simple supports. For the new boundary conditions, Fig. 7 shows the lateral deflections of the bottom flange corresponding to the same three different web thicknesses considered previously for the same 20 m span bridge. Compared with the previous case, drifts are smaller and longer PSa are needed to produce first yield. Hence, (6)–(11) can be used conservatively if expediency is desired.

Ultimate Nonlinear Behavior

The program ADINA (ADINA R&D 1995) was used to investigate the nonlinear behavior of these steel bridges and the

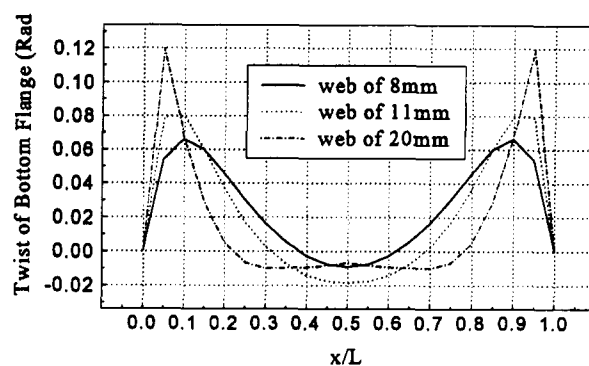


FIG. 6. Rotation of Girder Bottom Flange for 20 m Span Bridge (Simply Supported Laterally) for Normalized 100 mm of Maximum Transverse Displacement

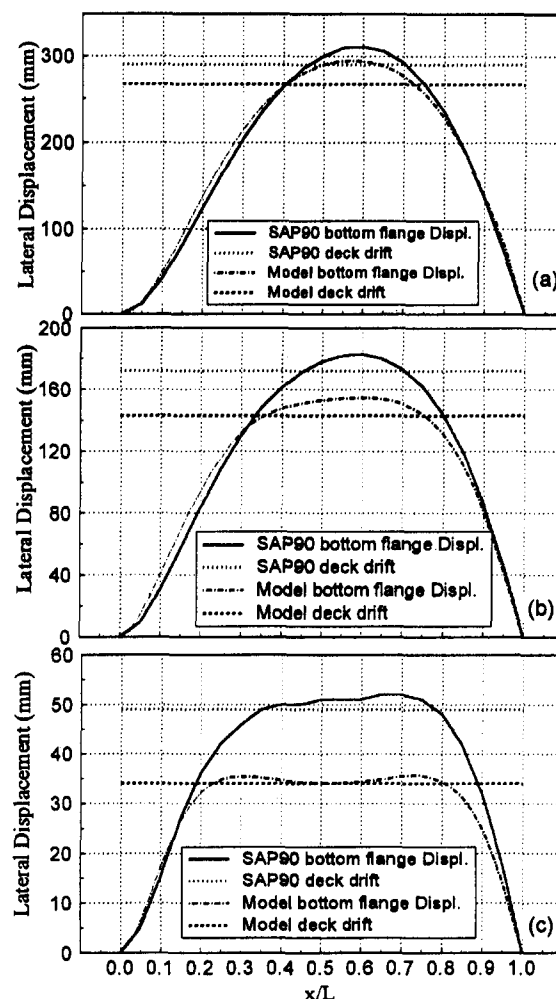


FIG. 7. Comparison of Girder Bottom Flange Displacements Obtained by SAP90 and Proposed Model for 20 m Span Bridge (Laterally Fixed at One End), Respectively, for Girder Web Thickness of (a) 8 mm; (b) 11 mm Corresponding to WWF800 × 184 in Original Design; (c) 20 mm

impact of $P-\Delta$ effects (second-order analysis) on this ultimate behavior. Results from push-over analyses shown in Fig. 8 indicate that, since lateral displacements are large in bridges without any diaphragms, $P-\Delta$ effects arising from the displaced weight of the deck are significant, leading to inelastic overturning and structural instability.

Inelastic analyses also revealed that, in the absence of end diaphragms, the presence of intermediate diaphragms does not greatly improve the seismic behavior of slab-on-girder bridges, since the largest girder web distortions occur near the girder

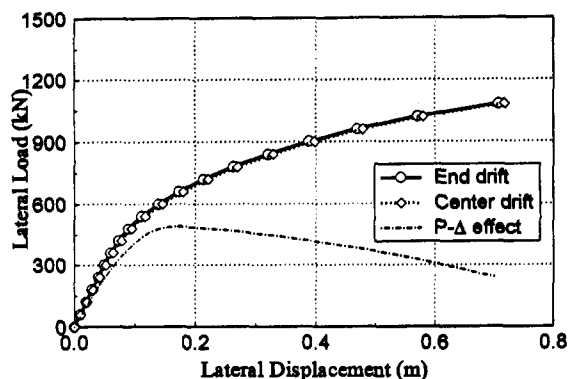


FIG. 8. Load-Displacement Curve for 40 m Span Bridge with and without Consideration of P-Δ Effect

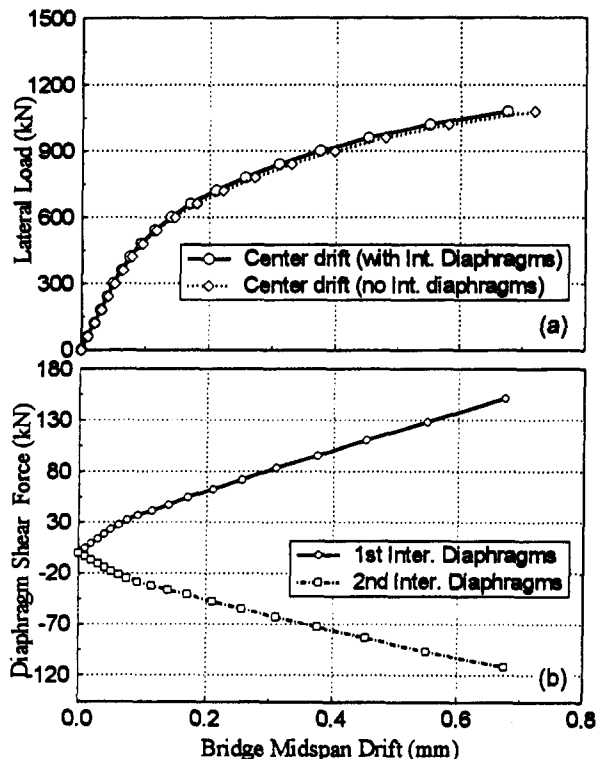


FIG. 9. Impact of Intermediate Diaphragms on 40 m Span Bridge without End Diaphragm: (a) Lateral Load versus Midspan Drift; (b) Horizontal Shear Force in Braces of First and Second Intermediate Diaphragms from Bridge End

supports. To illustrate this phenomenon, a 40 m span bridge with intermediate diaphragms at every 8 m was considered. As shown in Fig. 9, the impact of intermediate diaphragms in resisting the lateral loads is small. Note that as shown in Figs. 4, 5, and 7, the girder bottom flange can deform laterally further than the bridge deck in some locations. Consequently, the shear force resultant in some intermediate diaphragms can oppose that acting in the end diaphragms or other intermediate diaphragms [Fig. 9(b)].

Effect of Web Stiffeners

Typically, bearing web stiffeners are present (and needed) at the supports of steel bridge girders to prevent web crippling and web buckling under gravity loads. Most old existing bridges also have numerous intermediate transverse web stiffeners equally spaced along the length of girders and added to enhance the shear resistance of these girders. (The trend in new designs, however, is to avoid transverse stiffeners as much as possible.) In view of the structural seismic behavior de-

TABLE 2. Comparison of Elastic Lateral Deck Drift and Period of Steel Bridges, with and without Web Bearing Stiffeners, Subjected to 1g Pseudoacceleration*

| Bridge span (m) (1) | Web stiffeners size (2) | Lateral Drift (mm) | | Lateral Period (s) | |
|---------------------|-------------------------|---------------------|------------------------|---------------------|------------------------|
| | | With stiffeners (3) | Without stiffeners (4) | With stiffeners (5) | Without stiffeners (6) |
| 20 | 2P1. 100 × 10 | 5.3 | 228 | 0.11 | 0.94 |
| 30 | 2P1. 100 × 10 | 16 | 324 | 0.17 | 1.08 |
| 40 | 2P1. 100 × 10 | 30 | 478 | 0.26 | 1.27 |
| 50 | 2P1. 120 × 12 | 37 | 785 | 0.26 | 1.66 |
| 60 | 2P1. 120 × 12 | 56 | 1,195 | 0.30 | 2.03 |

*Assuming simply supported laterally.

scribed above, and recognizing the role played by the web of girders, some special considerations are necessary to account for the presence of these stiffeners.

First, without changes to the above theory, the effect of equally distributed intermediate transverse web stiffeners can be directly considered by converting each stiffened web into an equivalent unstiffened web having a thickness chosen to give an identical transverse flexural stiffness. For example, following this procedure, web stiffeners of 100 × 10 mm at spacing of 2 m on 11 and 16 mm thick webs (corresponding to 20 m and 60 m span bridges) can be converted into equivalent web thicknesses of 36 and 38 mm, respectively.

Second, when the bearing stiffeners at the supports are larger than the distributed intermediate web stiffeners (as they frequently are), they effectively contribute an additional stiffness at each support, essentially acting as end diaphragms, albeit weak ones. Finite element analyses were conducted to investigate the impact of this small effective end-diaphragm action. Table 2 presents the resulting maximum displacements and lateral period of vibration in steel bridges of different spans subjected to a lateral uniformly distributed load equivalent to a pseudo acceleration of 1g at the deck level. As indicated in this table, even though relatively small bearing web stiffeners were considered, their presence has a large impact on the lateral period and displacement of bridges.

As bearing stiffeners can effectively be treated as end diaphragms, it is worthwhile to extend the above analytical study to parametrically include the stiffness contribution of end diaphragms. This is done in the following.

SLAB-ON-GIRDER STEEL BRIDGES WITH EFFECTIVE DIAPHRAGMS

For bridges with diaphragms, preliminary analyses revealed that the concrete deck does not respond in a rigid-body motion during seismic excitations, as is the case for bridges without diaphragms. Rather, treating the structure as a generalized single degree of freedom (SDOF), it was found appropriate to express the transverse response displacement mode shape of the bridge, $u(x)$, by

$$u(x) = \sin \frac{\pi x}{L} \quad (13)$$

where L is the span length. The corresponding effective force, P_{eff} , acting on this system is calculated as (Clough and Penzien 1993)

$$P_{\text{eff}} = \frac{\zeta^2}{m^*} P S a = \frac{8m}{\pi^2} P S a \quad (14)$$

where m is the mass of the bridge; $P S a$ is the pseudo acceleration; and ζ , the earthquake excitation factor, is

$$\zeta = \int_0^L \frac{m}{L} u(x) dx = \frac{2m}{\pi} \quad (15)$$

It is noteworthy that, for the simplified equivalent system considered above, the effective force must act on the system, instead of $m^* \ddot{u}_g$. For instance, in a 60 m span bridge with a total mass of 465,000 kg, a P_{eff} of 3,700 kN, distributed along the bridge as a sine curve, is obtained from a pseudo acceleration of 1g, while in the case without diaphragms a lateral loading of 4,560 kN uniformly distributed along the bridge was previously considered for the same pseudo acceleration.

In the following, this effective force corresponding to a generic pseudo acceleration of 1g is considered, and as before, results from elastic analyses can be linearly scaled as necessary.

Proposed Model for Calculation of Period and Elastic Response

In the presence of end diaphragms, the model previously derived must be modified to properly capture the lateral response of this type of steel bridge. A new model that may account for the stiffness of end diaphragms, in addition to all the behavior features described earlier, is schematically illustrated in Fig. 10.

The following mathematical approach was followed to develop an analytical expression capturing the lateral behavior of these steel bridges under transverse seismic excitation.

The differential equation of motion for the bridge deck with continuous mass, neglecting the effects of shear strain and rotary inertia, can be written as (Gorman 1975)

$$-\frac{\partial^2 u(x, t)}{\partial t^2} = \frac{EI_D}{\rho A} \frac{\partial^4 u(x, t)}{\partial x^4} \quad (16)$$

where $u(x, t)$ is a displacement function of the bridge deck in terms of longitudinal distance from the support, x , and time, t ; I_D is the superstructure moment of inertia (slab and girders acting as a unit) about a vertical axis perpendicular to the deck; ρ is mass density; and A is the cross-sectional area of the entire superstructure. Hence, ρA corresponds to the superstructure mass per unit length. Using a displacement function of $u(x, t) = Z(t) \cdot Y(x)$ for bridge deck, the differential equation of motion becomes

$$-Y(x) \frac{d^2 Z(t)}{dt^2} = \frac{EI_D}{\rho A} Z(t) \frac{d^4 Y(x)}{dx^4} \quad (17)$$

This equation may be rearranged so that the left-hand side of the equality is a function of time only, while the other side is a function of distance, x :

$$-\frac{1}{Z(t)} \frac{d^2 Z(t)}{dt^2} = \frac{EI_D}{\rho A} \frac{1}{Y(x)} \frac{d^4 Y(x)}{dx^4} \quad (18)$$

By making both sides equal to a constant, say ω^2 , and then introducing a dimensionless parameter, α , defined as

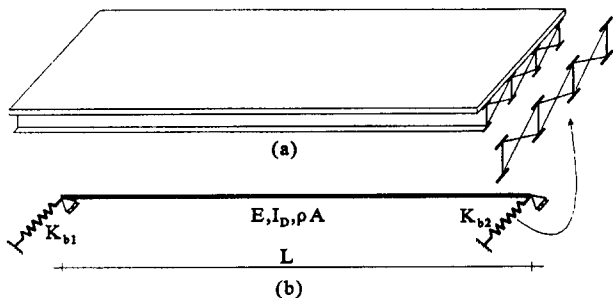


FIG. 10. Schematic Simplified Model for Bridges with End Diaphragms

$$\alpha^4 = \frac{\rho A \omega^2 L^4}{EI_D} \quad (19)$$

the following expressions for the general solution can be developed:

$$Y(x) = C_1 \sin \alpha x + C_2 \cos \alpha x + C_3 \sinh \alpha x + C_4 \cosh \alpha x \quad (20)$$

$$Z(t) = \cos(\omega t - \varphi) \quad (21)$$

where C_1 to C_4 are the coefficients depending on boundary conditions; and φ is a phase angle of the periodic motion. For a steel bridge having end diaphragms and assumed simply supported at both ends in the transverse direction, α can be obtained through trial and error by solving the following equality:

$$(K_b^*)^2 + \frac{\alpha^3(1 + C_k)(\sinh \alpha \cos \alpha - \sin \alpha \cosh \alpha)}{2C_k \sin \alpha \sinh \alpha} K_b^* + \frac{\alpha^6(1 - \cos \alpha \cosh \alpha)}{2C_k \sin \alpha \sinh \alpha} = 0 \quad (22)$$

where C_k is the ratio of right to left end-diaphragm stiffnesses (K_{b2}/K_{b1} , usually 1.0); and K_b^* , the dimensionless stiffness, is

$$K_b^* = \frac{K_b L^3}{EI_D} \quad (23)$$

in which K_b , the stiffness of lateral bracing systems at one end, depends on the geometry of the bridge and properties of the bearing stiffeners and diaphragm braces:

$$K_b = \sum_1^{n_g} \frac{12EI_s}{h_w^3} + \sum_1^{n_g-1} \frac{2EA_b \cos^2 \theta}{l_b} \quad (24)$$

where I_s is the moment of inertia of the bearing web stiffener about the longitudinal axis of the bridge; n_g is the number of girders; and A_b , l_b , and θ are the cross-sectional area, length, and slope angle of braces. It is noteworthy that, in the absence of diaphragm braces, K_b would simply be the lateral stiffness of transverse bearing web stiffeners, i.e., $\sum 12EI_s/h_w^3$. For example, with two-sided P1. 100 × 10 only, in a 20 m span bridge of four girders, I_s and K_b would be $7.8 \times 10^{-6} \text{ m}^4$ and 170 kN/mm, respectively. With X-shape braces of 2L100 × 100 × 10 between every two girders at bridge ends, K_b would be 1,930 kN/mm (neglecting the contribution of the bearing stiffeners), and K_b^* would be 55.33, giving α of 2.71 [see (22)], considering I_D and ρA of 1.322 m^4 and 6,300 kg/m, respectively, this would correspond to a lateral period of 0.053 s [per (19)]. Note that if rocking of the girders on the end bearing occurs, the term $\sum 12EI_s/h_w^3$ should be replaced with $\sum 3EI_s/h_w^3$; rocking at the top of a noncomposite girder would further reduce the contribution of transverse bearing web stiffeners to lateral load resistance.

On the other hand, if the girders' bottom flange lateral support conditions at one end of the simply supported bridge are considered fixed, then assuming $C_k(K_{b2}/K_{b1})$ to be 1.0, (22) becomes

$$\frac{(K_b^*)^2}{\alpha^6} (\sinh \alpha \cos \alpha - \sin \alpha \cosh \alpha) - \frac{K_b^*}{\alpha^3} (1 + 3 \cos \alpha \cosh \alpha) + \sin \alpha \cosh \alpha + \sinh \alpha \cos \alpha = 0 \quad (25)$$

For the same 20 m span bridge, α would be 2.96, giving a lateral period of 0.044 s.

In all cases, the displacement at the bridge ends is given by

$$\Delta_{end} = \frac{m \cdot (PSa)}{K_{b1} + K_{b2}} \quad (26)$$

Rayleigh's method can be used alternatively to the proposed approach to calculate the period of these bridges, considering the bridge as a beam with continuous mass and elastic springs at the supports. This approach is a specific case of the method of generalized coordinates in which the shape function is determined on the basis of the static displacement of structure. The maximum potential and kinetic energies, V_{\max} and T_{\max} , can generally be integrated from the following equations:

$$V_{\max} = \frac{1}{2} \int_0^L m(x)g u(x) dx \quad (27a)$$

$$T_{\max} = \frac{1}{2} \omega^2 \int_0^L m(x)(u(x))^2 dx \quad (27b)$$

where $u(x)$ is the lateral displacement function assumed for the bridge; L and $m(x)$ are span length and distributed mass of the bridge; g is gravitational acceleration; and ω is the transverse frequency in rad/s. By equating the two energies,

$$\omega^2 = g \frac{\int_0^L m(x)u(x) dx}{\int_0^L m(x)[u(x)]^2 dx} \quad (28)$$

For a 20 m span simply supported bridge having only two web stiffeners of 100×10 size at each support, ω is computed as 57 rad/s from the above formula, corresponding to a lateral period of 0.11 s. By adding $2L100 \times 100 \times 10$ braces to the ends, the lateral period decreases to 0.052 s if simply supported laterally and to 0.043 s in the presence of a fixed support. These results compare well with those obtained by SAP90.

Numerical Examples

Using SAP90, the lateral period was computed for bridges with different spans, considering various X braces as diaphragms. Note that many of the bridges' lower modes of vibration correspond to displacement response in the vertical direction. The discussion here addresses the lateral period corresponding to lateral response.

Fig. 11 shows the resulting lateral period versus brace cross-sectional area for 20, 40, and 60 m span bridges. If a zero cross-sectional area is assumed for the braces, periods of 0.82 and 1.77 s are obtained, respectively for 20 and 60 m long bridges, i.e., the same values obtained before. By using $2L45 \times 45 \times 5$ and $2L100 \times 100 \times 10$ X braces, lateral periods of 0.089 and 0.052 s are obtained for the 20 m span bridge, and 0.24 and 0.22 s, respectively, for the 60 m span bridge. It is observed that a very small end diaphragm is sufficient to

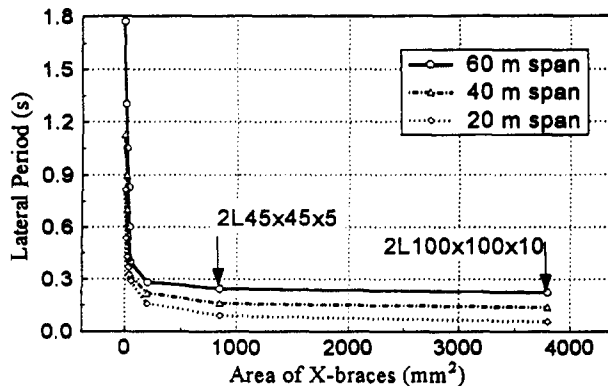


FIG. 11. Lateral Period versus Cross-Sectional Area of Braces for 20, 40, and 60 m Span Bridges (Laterally Fixed at One End)

TABLE 3. Lateral Periods of Braced Bridges Obtained by Proposed Method and SAP90*

| Bridge span (m) | ρA (kg/m) | I_b (m ⁴) | X-brace size | T_{SAP90} (s) | $T_{proposed}$ (s) | Difference (%) |
|-----------------|-----------------|-------------------------|------------------|-----------------|--------------------|----------------|
| (1) | (2) | (3) | (4) | (5) | (6) | (7) |
| 20 | 6,300 | 1.322 | 2L100 × 100 × 10 | 0.0515 | 0.047 | 8 |
| 30 | 6,733 | 1.617 | 2L100 × 100 × 10 | 0.076 | 0.071 | 7 |
| 40 | 7,150 | 1.797 | 2L100 × 100 × 10 | 0.12 | 0.112 | 6.6 |
| 50 | 7,340 | 1.983 | 2L100 × 100 × 10 | 0.17 | 0.16 | 6 |
| 60 | 7,750 | 2.212 | 2L100 × 100 × 10 | 0.222 | 0.213 | 4 |

*It is assumed there is one laterally fixed end; ρA is the superstructure mass per unit length.

produce a large "shift" in the period of these bridges, but that further increases in diaphragm stiffness have only a marginal impact on lateral structural period.

Table 3 presents the lateral periods for all braced bridges considered in this study and compares them with the periods obtained by SAP90. The difference between the results is smaller for larger span bridges, because shear deformations of the concrete deck are ignored in the proposed analytical model. For the 60 m span bridge, where the shear to flexural deformation ratio is the lowest, the proposed hand-calculation analytical model offers the results closest to those obtained by SAP90.

Ultimate Nonlinear Behavior

Frequently, end diaphragms have sufficient strength to remain elastic during earthquakes, and brittle damage instead occurs in the diaphragm connections or elsewhere in the structure. However, to investigate whether intermediate diaphragms can effectively contribute to lateral load resistance when end diaphragms undergo inelastic response, inelastic push-over analyses were carried out using ADINA. Results are shown in Fig. 12 for 40 and 60 m span bridges having X-brace diaphragms between the girders, namely $2L65 \times 65 \times 6$ for end diaphragms and $2L45 \times 45 \times 5$ for intermediate diaphragms. Three pairs of braces are present in each diaphragm. The contribution resisted by flexure of the stiffened girders [per (24)] is not shown. As shown in Fig. 12, intermediate diaphragms take only a small percentage of the total applied load, even after buckling and yielding of the end-diaphragm braces, and would remain elastic until very large ductilities developed in the end diaphragms and at least until deck drifts in excess of 5%. The contribution of intermediate diaphragms is even less significant for the shorter bridges. This is because intermediate diaphragms are located 8 m from each other, the first one being at a greater percentage of the total span from the end in shorter bridges, and thus less likely to contribute, being more remote from the zone of greater girder transverse deformation.

Note that results previously obtained for bridges without end diaphragms and presented earlier should be used if end diaphragms are deemed incapable of developing the ductile behavior assumed here.

Further Observations on Seismic Behavior

Deformed shapes for a 40 m span bridge at one end and at a distance of 8 m from the end are shown in Fig. 13. It is noteworthy that even though the lateral inertia force is applied at the deck level and that supports are provided only at the level of the lower bottom flanges at the bridge end, the bridge deck rotates conversely to the direction of the resulting couple, or counterclockwise at the middle. This is due to the axisymmetric cross section of the bridge, which has a shear center located above the concrete slab.

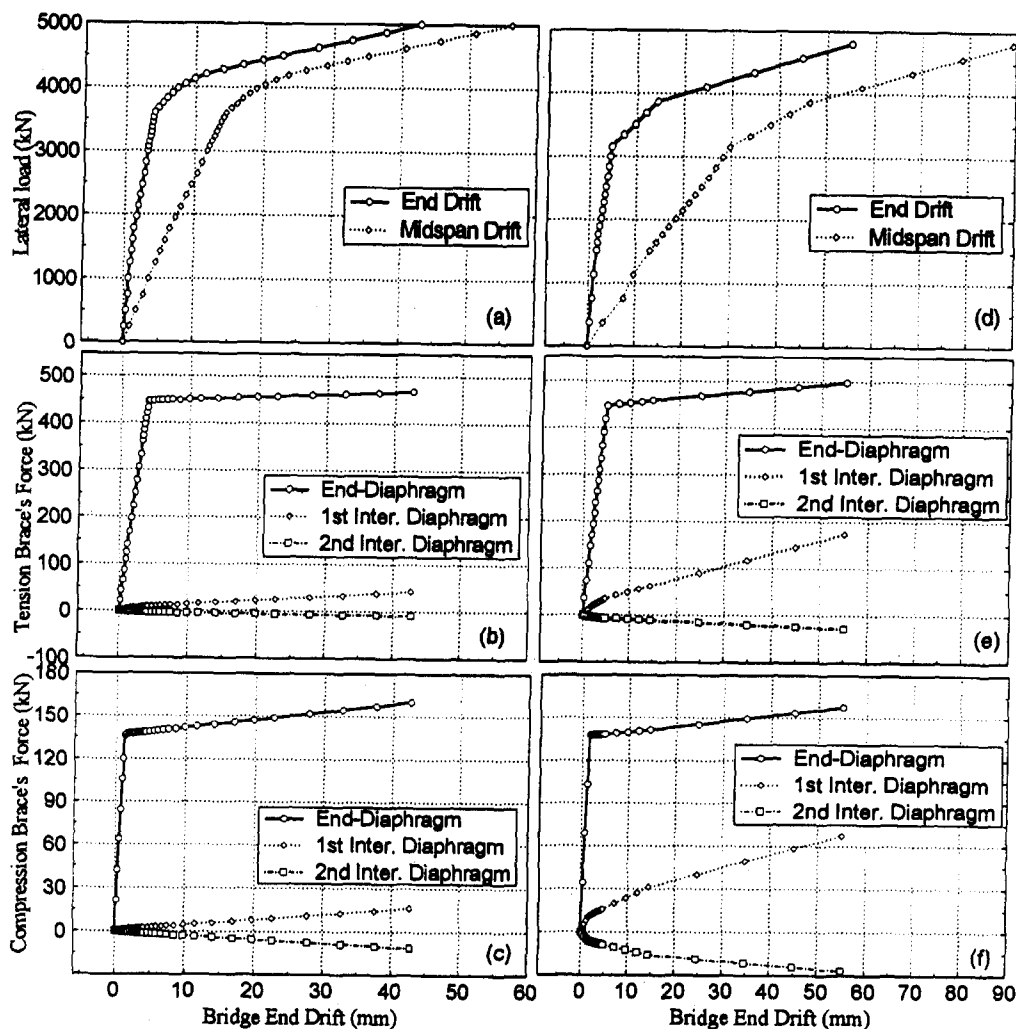


FIG. 12. (a) and (d) Lateral Loads Imposed to Braced 40 and 60 m Span Bridges, Respectively, versus End and Midspan Drifts; (b) and (c) Tension and Compression Axial Forces in One Pair of Diaphragm Braces for 40 m Span Bridge; (e) and (f) Same for 60 m Span Bridge

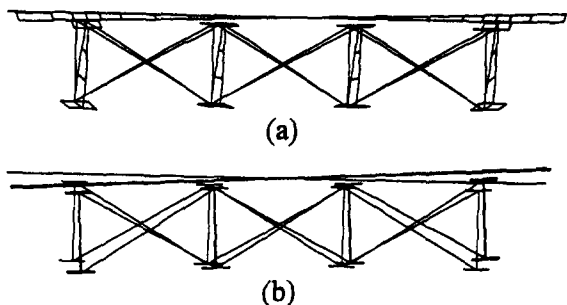


FIG. 13. End Views of Deformed Shapes for 40 m Span Bridge at (a) One End; (b) Distance of 8 m from Bridge End

CONCLUSIONS

Linear elastic and nonlinear inelastic analyses were conducted to investigate the impact of diaphragms on the seismic behavior of straight slab-on-girder steel bridges. The results of this limited analytical study demonstrate that a small end-diaphragm stiffness is sufficient to make the entire superstructure behave as a unit in the elastic range. However, the above results also illustrate that a dramatic shift in seismic behavior could occur once rupture of the end diaphragms occurred, with a sizable period elongation, considerably larger lateral displacements, and a higher propensity to damage in response to instability and $P-\Delta$ effects. It is also found that the presence of intermediate diaphragms does not significantly influence the

seismic performance of these bridges, both in the elastic and inelastic range, regardless of whether end diaphragms are present or not.

Moreover, these analyses confirmed that effective end diaphragms constitute critical structural elements along the main seismic load path, and that they should be designed accordingly. Therefore, in new bridges, they should be designed to resist in an elastic manner the forces induced by the maximum credible earthquake. Alternatively, they could be designed and detailed as ductile members to preclude brittle member or connections failure. This is not warranted for intermediate diaphragms. Nonductile end-diaphragm members and connection details in existing steel bridges should be retrofitted, because of their impact on seismic response.

ACKNOWLEDGMENTS

The Natural Sciences and Engineering Research Council of Canada is acknowledged for its financial support through Strategic and Collaborative Grants on the Seismic Evaluation of Existing Bridges. Also, the scholarship of the first writer from the Ministry of Culture and Higher Education of Iran is highly appreciated. The findings and recommendations in this paper are those of the writers, and not necessarily those of the sponsors.

APPENDIX. REFERENCES

AASHTO LRFD bridge design specifications—SI (metric). (1994). American Assoc. of State Highway and Transp. Officials, Washington, D.C.

- ADINA R&D, Inc. (1995). "Automatic dynamic incremental nonlinear analysis." Watertown, Mass.
- Applied Technology Council. (1981). "Seismic design guidelines for highway bridges." *Rep. ATC-6*, Redwood City, Calif.
- Astaneh-Asl, A., Bolt, B., McMullin, K. M., Donikian, R. R., Modjtahedi, D., and Cho, S. W. (1994). "Seismic performance of steel bridges during the 1994 Northridge earthquake." *UCB Rep. CE-STEEL 94/01*, Univ. of California, Berkeley, Calif.
- Azizinamini, A., Kathol, S., and Beacham, M. (1995). "Influence of cross frames on load resisting capacity of steel girder bridges." *AISC Engrg. J.*, 32(3), 107–116.
- Bruneau, M., Wilson, J. W., and Tremblay, R. (1996). "Performance of steel bridges during the 1995 Hyogo-ken Nanbu (Kobe, Japan) earthquake." *Canadian J. Civ. Engrg.*, Ottawa, Canada, 23(3), 678–713.
- Buckle, I. G., Mayes, R. L., and Button, M. R. (1986). "Seismic design and retrofit manual for highway bridges." Computech Engineering Services, Berkeley, Calif. Published also as *Rep. FHWA-IP-87-6*, U.S. Dept. of Transp., Federal Highway Administration, Washington, D.C.
- Clough, R. W., and Penzien, J. (1993). *Dynamics of structures*. McGraw-Hill Book Co., Inc., New York, N.Y.
- Dicleli, M., and Bruneau, M. (1995). "Seismic performance of multi-span simply-supported slab-on-girder steel highway bridges." *Engrg. Struct.*, 17(1), 4–14.
- Dicleli, M., and Bruneau, M. (1996). "Quantitative approach to rapid seismic evaluation of slab-on-girder steel highway bridges." *J. Struct. Engrg.*, ASCE, 122(10), 1160–1168.
- Earthquake Engineering Research Institute. (1990). "Loma Prieta earthquake reconnaissance report." *Spectra*, supplement to vol. 6, Oakland, Calif.
- Earthquake Engineering Research Institute. (1994). "Northridge Earthquake Jan. 17, 1994, preliminary reconnaissance report." Oakland, Calif.
- Gorman, D. J. (1975). *Free vibration analysis of beams and shafts*. John Wiley & Sons, Toronto, Canada.
- Kawashima, K. (1990). "Seismic design, seismic strengthening and repair of highway bridges in Japan." *Proc., First U.S.-Japan Workshop on Seismic Retrofit of Bridges*, Tsukuba Science City, Japan.
- Mitchell, D., Bruneau, M., Williams, M., Anderson, D., Saatcioglu, M., and Sexsmith, R. (1995). "Performance of bridges in the 1994 Northridge earthquake." *Canadian J. Civ. Engrg.*, Ottawa, Canada, 22, 415–427.
- Ontario highway bridge design code. (1991). Ministry of Transp., Quality and Standards Division, Ontario, Canada.
- Roberts, J. E. (1992). "Sharing California's seismic lessons." *Modern steel construction*, 32–37.
- Standard specifications for highway bridges. (1961). American Association of State Highway Officials, Washington, D.C.
- Standard specifications for highway bridges, 15th Ed. (1994). American Assoc. of State Highway and Transp. Officials, Washington, D.C.
- Tseng, W. S., and Penzien, J. (1973). "Analytical investigations of the seismic response of long multiple-span highway bridges." *EERC Rep. 73-12*, Univ of Calif., Berkeley, Calif.
- Wilson, E. L., and Habibullah, A. (1992). "SAP90 computer software for structural & earthquake engineering." Computers & Structures Inc., Berkeley, Calif.